Preliminary results for the design, fabrication, and performance of a backside-illuminated avalanche drift detector*

Qiao Yun(乔 赟), Liang Kun(梁 琨)†, Chen Wen-Fei(陈文飞), and Han De-Jun(韩德俊)

The Key Laboratory of Beam Technology and Materials Modification of the Ministry of Education, College of Nuclear Science and Technology, Beijing Normal University, Beijing 100875, *China*

(Received 2 August 2013; revised manuscript received 14 August 2013)

The detection of low-level light is a key technology in various experimental scientific studies. As a photon detector, the silicon photomultiplier (SiPM) has gradually become an alternative to the photomultiplier tube (PMT) in many applications in high-energy physics, astroparticle physics, and medical imaging because of its high photon detection efficiency (PDE), good resolution for single-photon detection, insensitivity to magnetic field, low operating voltage, compactness, and low cost. However, primarily because of the geometric fill factor, the PDE of most SiPMs is not very high; in particular, for those SiPMs with a high density of micro cells, the effective area is small, and the bandwidth of the light response is narrow. As a building block of the SiPM, the concept of the backside-illuminated avalanche drift detector (ADD) was first proposed by the Max Planck Institute of Germany eight years ago; the ADD is promising to have high PDE over the full energy range of optical photons, even ultraviolet light and X-ray light, and because the avalanche multiplication region is very small, the ADD is beneficial for the fabrication of large-area SiPMs. However, because of difficulties in design and fabrication, no significant progress had been made, and the concept had not yet been verified. In this paper, preliminary results in the design, fabrication, and performance of a backside-illuminated ADD are reported; the difficulties in and limitations to the backside-illuminated ADD are analyzed.

Keywords: avalanche drift detector, silicon photomultiplier, photon detection efficiency, photon detector

PACS: 85.60.Gz, 85.60.Ha, 85.60.Bt, 85.60.Dw **DOI:** 10.1088/1674-1056/22/10/108504

1. Introduction

Research into the silicon photomultiplier (SiPM), which is a matrix structure of Geiger-mode avalanche photodiodes (GAPDs)[1] and is known as a multi-pixel photon counter (MPPC),[2] for photon detection has made great progress.[3] Recently, the SiPM has become an alternative to the photomultiplier tube (PMT)[4] in high-energy physics (HEP), astroparticle physics, and positron emission tomography (PET) due to the outstanding characteristics of the SiPM: high photon detection efficiency (PDE), good resolution for single-photon detection, low sensitivity against temperature, and bias fluctuations, lack of aging over years,[5] insensitivity to magnetic fields, low operating voltage, compactness, and convenience for integration.[6] Although the SiPMs reported by some institutes and companies have unique advantages, SiPMs cannot always meet the various requirements of experiments and applications. In many applications, SiPMs are used to detect low-level light over a wide wavelength range. Limited by the fill factor, the PDE of most available SiPMs is low or is only high for the incident light in a narrow wavelength range. SiPMs with small pixel sizes and large pixel densities have large dynamic ranges but have low PDE. Additionally, the dark rate of SiPM is relatively high because of thermally generated carriers and the leakage current of the P–N junction.[7] If the size of the detector is increased, the dark rate will accordingly be significant. To solve these shortcomings of SiPMs, the backside-illuminated avalanche drift detector (ADD) began to be studied for serving as a building block for SiPMs.

The concept of the backside-illuminated ADD was first proposed by Vilkelis *et al.*[8] in 2001. To meet the requirements of single-photon detectors for application in the Major Atmospheric Gamma-ray Imaging Cherenkov telescopes (MAGIC), in 2005, researchers in the Max Planck Institute (MPI) for Physics in Germany developed the concept of the ADD,[8] which combines a drift diode with an avalanche structure placed on the opposite side of the irradiation entrance window. The ADD should have high PDE and large receive area while restricting the avalanche region to a very small area of the device. As shown in Fig. 1, the structure designed by the MPI has a modulated high field region between the deep p and the deep n regions. In fact, it is difficult to ensure that the deep p region is fully depleted when avalanche multiplication occurs, thus part of the deep p region remains neutral, and most photoelectrons have been recombined in the neutral region before they enter the modulated high field region to trigger the avalanche process. This recombination might be one reason that only simple test structures and simulation results have been reported by the MPI to date.[9]

*Project supported by the National Natural Science Foundation of China (Grant No. 11005010).

†Corresponding author. E-mail: lk@bnu.edu.cn

© 2013 Chinese Physical Society and IOP Publishing Ltd

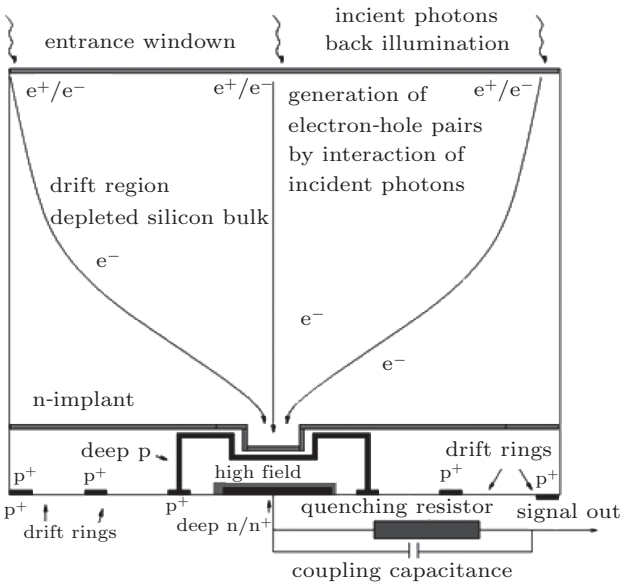


Fig. 1. The basic structure and working principle of the backside-illuminated SiPMs of the MPI.[7]

The Novel Devices Laboratory (NDL) of Beijing Normal University has long been committed to investigating silicon photomultipliers with bulk integrated quenching resistors and silicon drift detectors. Replacing the "point-like" collecting anode of a silicon drift detector (SDD) with a one-sided abrupt junction, a developed structure for the backside-illuminated ADD was proposed by the NDL. The developed structure differs from the MPI's ADD structure, in which the photoelectrons generated in the depleted bulk barely enter into the high field region and fail to trigger avalanche multiplication.

The backside-illuminated ADD designed by the NDL is expected to have a promising PDE, low dark rate, and detect low-level light over a wide wavelength range, and be conveniently integrated into novel large-area SiPMs. Compared with the ADD of the MPI, the newly developed structure is simple, and the avalanche junction has single electrode. In this paper, the preliminary results from the investigation of the backside-illuminated ADD developed at the NDL are presented. The validity of the developed structure is first demonstrated in device simulations. Through the use of a planar silicon detector processing line, the production of the complete structure of the backside-illuminated ADD is accomplished. The electrical and the photoelectric performances of the fabricated ADD are characterized. Finally, through the experimental studying and the theoretical analysis, the limitations and prospects for the development of the backside-illuminated SiPMs are discussed.

2. Structure and principles

The basic structure of the backside-illuminated avalanche drift detector designed by the NDL and the operational principle are shown in Fig. 2. The volume of the device is 150 μm×150 μm×300 μm; the size of the back entrance window is 110 μm×110 μm; the diameter of the "point-like" avalanche junction is 12 μm.

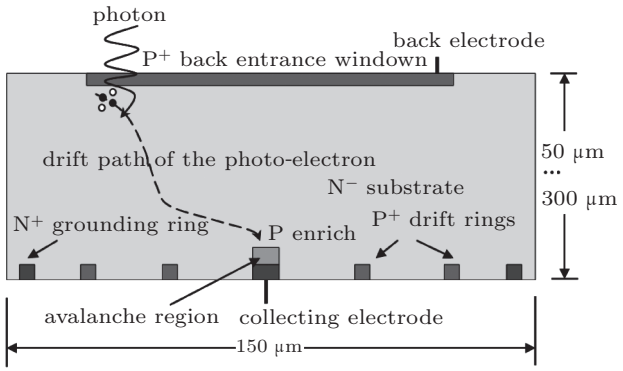


Fig. 2. Structure and operational principle of the newly developed backside-illuminated ADD of the NDL.

Under appropriate conditions, the n-type silicon bulk, in which a drift electric field has a strong component parallel to the surface, is fully depleted. The drift electric field generated by the front-side drift rings and the back electrode drives the signal photo-electrons towards the central small-size avalanche diode. Through biasing at the collecting electrode, a high field region forms between the N^+ collecting electrode and the P enriched region. With high reverse bias at breakdown, the central N^+–P junction operates in Geiger mode. Low-level light illuminates the unstructured back entrance window, and the incident photons are converted into electron–hole pairs in the fully depleted n-type silicon bulk. The photo-electrons drift along the path and enter into the high field region to trigger avalanche multiplication. The electrical signal can be detected from the circuit connected to the N^+ collecting electrode. The photo-generated holes and the diffusion holes are swept into the P^+ drift rings and the P^+ back electrode.

The back entrance window is in the unstructured P–N junction, which provides homogeneous sensitivity over the entire active area of the detector. The backside-illuminated ADD guarantees a 100% fill factor because the optical window is unstructured and has no dead zone. Therefore, this structure can improve the PDE. Because the size of the avalanche region is much smaller than that of the active region, the detector has large pixels but meanwhile low dark rate. Because the photoelectrons can be generated in the whole substrate, the light absorption length is approximately equal to the thickness of the wafer, and the wide response wavelength range is promised to be achieved. If the backside-illuminated ADDs are integrated into a novel SiPMs, the SiPMs can be expected to have excellent PDE, low dark rate, excellent resolution for single-photon detection, and wide spectral response.

3. Simulations

Device simulations have been performed with ISE-TCAD release 10.0 for the structure with a radius of 150 μm and a thickness of 100 μm as shown in Fig. 2. For the ADD under the simulation conditions, the bulk is fully depleted and the drift electric field is formed. The simulation conditions include applied voltages of −0.8 V, −10.0 V, and −6.8 V to the inner drift ring, the outer drift ring and the back electrode, respectively. Meanwhile, the N^+ collecting electrode is biased at 30 V to keep the avalanche junction in Geiger mode.

The electrostatic potential distribution and the electron current density are both simulated. In the electrostatic potential distribution shown in Fig. 3, the (black) thick line indicates the electronic potential valley, which determines the drift path of the photo-electrons in the fully depleted silicon bulk of the presented structure. Definitely, the electron current flows along the drift path.

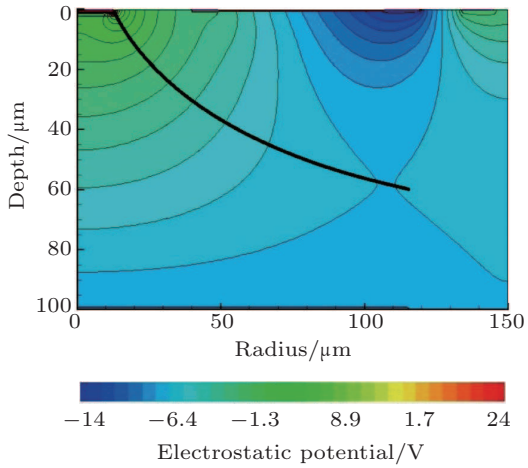


Fig. 3. (color online) Electrostatic potential distribution of the structure shown in Fig. 2 under the simulation conditions. The black (thick) line indicates the electronic potential valley.

Magnified views of the simulated distribution in the central region of electric field, electron current, and hole current density are presented in Figs. 4–6, in which the depth between 0.2 μm and 0.6 μm represents the N^+ region; the depth between 0.6 μm and 2.2 μm represents the P-enriched region; and the region deeper than 2.2 μm is in the N substrate. The high field region shown in Fig. 4 is located at the reverse-biased N^+–P junction formed between the N^+ region and the P-enriched region, which is not in the corner of the regions. The maximum electric field reaches more than 5×10^5 V/cm at the interface between two regions. The electron current shown in Fig. 5 is mainly distributed in the N^+ region, the upper part of the P-enriched region and the depleted bulk, but is not across the P-enriched region. The hole current shown in Fig. 6 is mainly distributed in the high field region and the zone beneath the high field region, in which there is a forward-biased P–N junction formed between the P-enriched region and the N substrate. The hole current flows to the substrate through the forward-biased P–N junction.

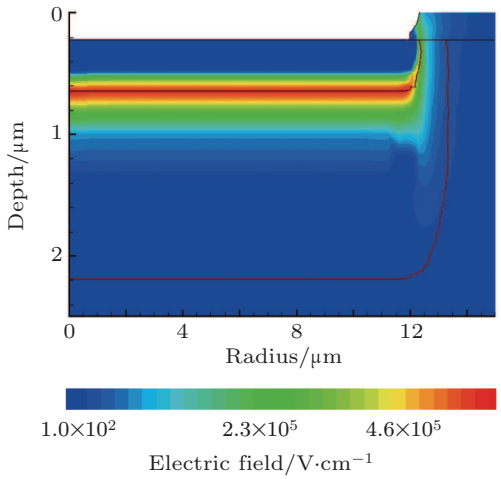


Fig. 4. (color online) Electric field distribution in the central avalanche region. The ADD is under the simulation conditions.

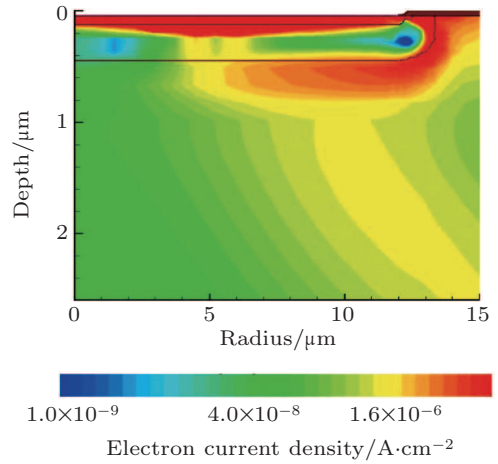


Fig. 5. (color online) Electron current density distribution in the central region. The ADD is under the simulation conditions.

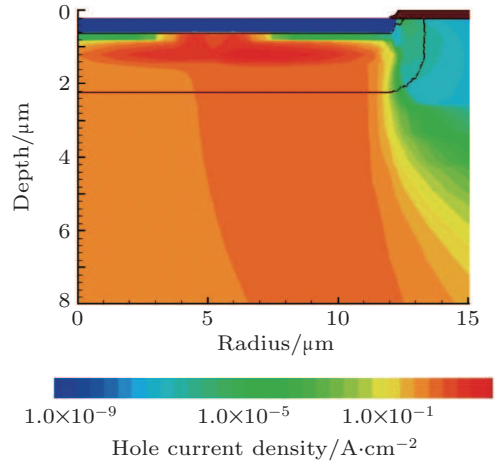


Fig. 6. (color online) Hole current density distribution in the central region. The ADD is under the simulation conditions.

The device simulations show that the presented ADD structure is feasible.

4. Experiment

4.1. Fabrication

Based on the planar silicon detector processing line at the NDL, the backside-illuminated ADD with a size of 150 μm×150 μm×300 μm and an active area of 110 μm×110 μm are fabricated. We choose an n-type ⟨111⟩ float zone silicon wafer polished on both sides; the resistivity of the wafer is 6000 Ω·cm–25900 Ω·cm, and the thickness is 300 μm.

The main technological processes shown in Fig. 7 include (i) growth of SiO_2 by thermal oxidation; (ii) opening SiO_2 window at the central collecting electrode by lithography and etching; (iii) boron ion implantation at different doses and phosphorus ion implantation at large doses to form the avalanche junction; (iv) fabrications of the drift rings and the back entrance window by double-sided lithography with infrared alignment and double-sided implantation of boron ions at low energy and large doses; (v) fabrications of the grounding ring by lithography, etching, and phosphorus ion implantation; (vi) double-sided metallisation for the Ohmic contacts.

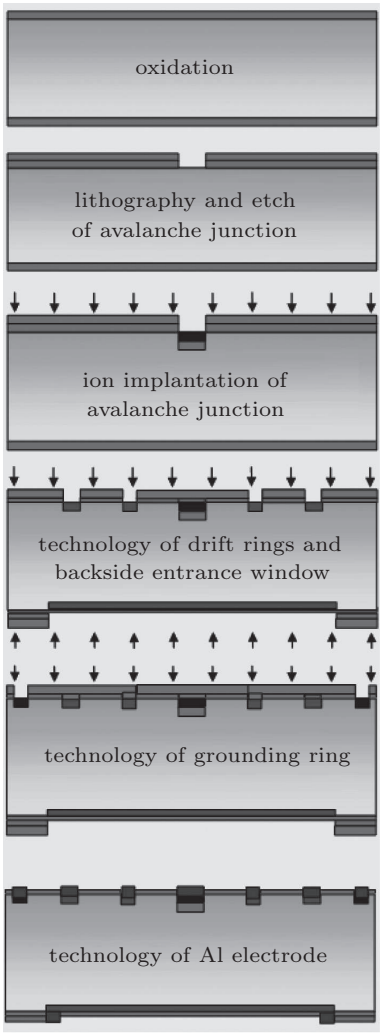


Fig. 7. Fabrication of the backside-illuminated ADD.

The fabrication of the backside-illuminated ADD is very complex due to the double-sided structure. Double-sided parallel technology is employed to reduce the difficulty and to improve the efficiency of the production.

After the technological process is completed, the detectors on the chips are selected, then removed from the chip, and finally encapsulated within To-8 shells. For the backside-illuminated ADD, the chip checking and encapsulation are difficult and complex due to the double-sided structure and multiple electrodes. A photo of the encapsulated ADD is shown in Fig. 8.

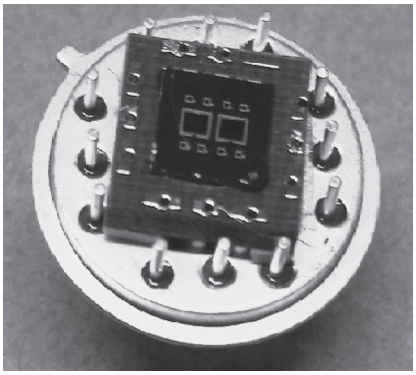


Fig. 8. Encapsulated backside-illuminated ADD.

4.2. Characterisation

The characteristics include the direct current properties and the photoelectric performances. All the tests are performed at room temperature.

An Agilent 4156C Precision Semiconductor Parameter Analyzer or a Keithley 237 Source-Measure Unit is used to measure the current–voltage (I–V) characteristics.

The photoelectric performances are measured after the device has been encapsulated. The ADD without an additional quenching resistor must be appropriately biased. At this point, the avalanche junction is operated in Geiger mode and the avalanche pulse is generated. The signal from the collecting electrode is amplified by the charge-sensitive preamplifier and the main amplifier, and then is observed on the oscilloscope. The dark avalanche pulse is measured. For analyzing the count rate of the photo-induced avalanche pulse, the count rate of the dark avalanche pulse is considered as a reference rate.

To study the optical response, an ordinary solar spectrum lamp in the NDL, an infrared laser with a wavelength of 850 nm, and a green light-emitting diode (LED) with a wavelength of 525 nm are used to illuminate the entrance window of the ADD respectively, through a fibre probe with a diameter of 120 μm. By using a function generator to drive the laser or the LED, the incident light intensity and the frequency can be modulated.

5. Results

The typical *I–V* characteristics of the avalanche junction of the fabricated ADD are shown in Fig. 9, in which double inflection point appears and indicates the self-quenching mechanism. The leakage current is less than 0.1 nA; the breakdown voltage is approximately 25 V.

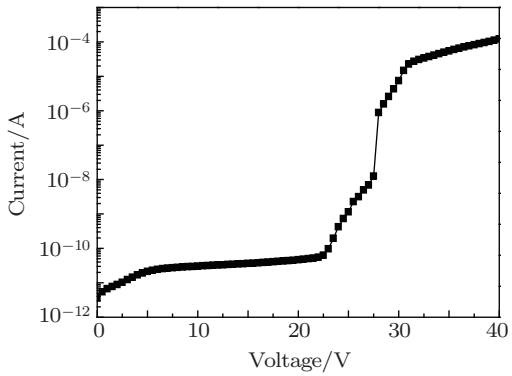


Fig. 9. Typical *I–V* characteristics of the avalanche junction of a fabricated backside-illuminated ADD.

The avalanche junction is characterized while the inner, outer drift rings, and the back electrode are biased at −0.3 V, −6.4 V, and −18.0 V, respectively. It is the typical operating condition. Additionally, the collecting electrode is biased at 27 V to ensure that the avalanche junction is operated in Geiger mode.

The dark pulse is measured for the ADD under the typical operating conditions. The count rate shown in Fig. 10 is only 6.5 kHz. The size of the avalanche junction is much smaller than that of the active region; therefore, the ADD has a low dark rate and low dark current.

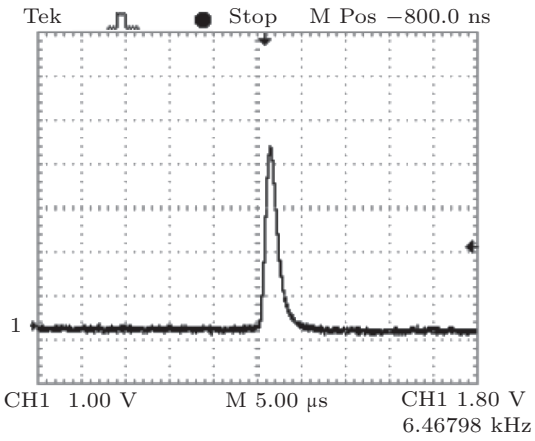


Fig. 10. Dark pulse of the fabricated backside-illuminated ADD under the typical operating conditions.

The detector is illuminated with the pulsed light, and the experimental results are shown in Figs. 11 and 12.

For the case of Fig. 11, the green LED is triggered at a frequency of 1 MHz. When the driving voltage increases, the incident light intensity and the avalanche pulse counts increase correspondingly; however, the count of the photo-induced avalanche pulses is low and the highest count is 20 kHz only. The photo-induced avalanche pulse reduces the amplitude as the incident light intensity increases.

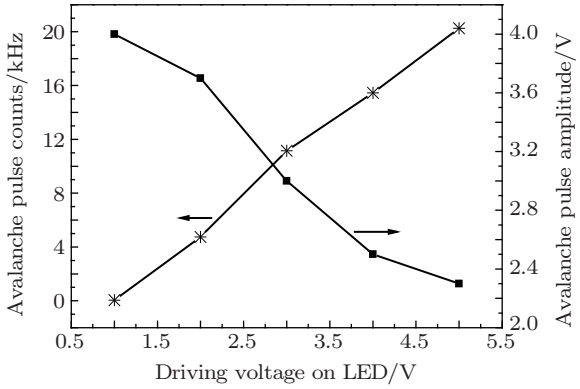


Fig. 11. Variations of the count and the amplitude of the photo-induced avalanche pulse with driving voltage on LED, whose driving frequency is fixed at 1 MHz. The ADD is under the typical operating conditions.

The avalanche pulse count shown in Fig. 12 apparently increases as the triggering frequency increases, with the driving voltage fixed at 3 V. For the triggering frequency above 1 MHz, the avalanche pulse count begins to decrease.

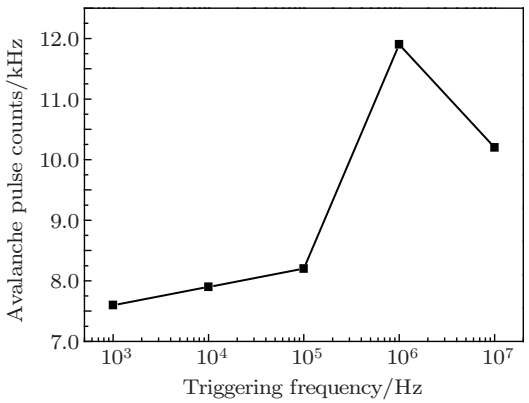


Fig. 12. Variation of the avalanche pulse count with triggering frequency at LED, whose driving voltage is 3 V. The ADD under the typical operating conditions.

6. Discussion

Based on the simulations and analysis, the experimental results on the backside-illuminated ADD of the NDL are discussed as follows.

Firstly, the self-quenching mechanism can be explained by analyzing the electric field and the current density distribution. The conclusion is that the avalanche process is quenched by the change in the electric field. As shown in Fig. 4, avalanche multiplication first takes place at the reverse-biased N^+–P junction, which operates in Geiger mode, without illumination. The multiplied electrons are collected by the collecting electrode. Meanwhile, the multiplied holes are collected by the forward-biased P–N junction beneath the N^+–

P junction, because it acts as a potential well of approximately 0.5 V–0.7 V. If the accumulation of holes in the potential well leads to a sharp decrease in electric field in the avalanche region, the avalanche process in the N^+–P junction will be quenched. After that the avalanche process is stopped; the accumulated holes drift into the substrate and are finally collected by the N–P^+ junction formed between the substrate and the back electrode or the drift rings. Therefore, the dark avalanche pulse is observed in characterization of the presented ADD without an additional quenching resistor.

Under illumination, the incident photons enter into the depleted bulk through the entrance window and generate electron–hole pairs. There has been a rise in the concentration of holes in the substrate. Many multiplied holes generated in the avalanche process cannot diffuse from the P-enriched region into the N substrate; as a result, the potential in the P-enriched region is raised. Since the applied voltage to the collecting electrode is unchanged, the electric field intensity in the N^+–P avalanche junction is reduced. Consequently, the amplitude of the avalanche pulse decreases, which is in accordance with the variation trends shown in Fig. 11. If the incident light intensity continues to increase, the electric field will become too low to trigger avalanche multiplication, and the photo-induced avalanche pulse will disappear.

The photoelectrons generated in the silicon bulk are driven by the drift field along the drift path shown in Fig. 3, and then enter into the N^+ region, where the positive voltage is maximized. For a one-sided abrupt junction, the high field region is primarily located on the side with low dopant concentration. Thus, the high field region of the avalanche junction is distributed on the P-enriched side. Most of the photo-electrons drifting to the N^+ region are directly removed by the collecting electrode, and they do not pass through the high electric field region. Only a few electrons enter into the high field region and trigger avalanche multiplication. Therefore, the counts of the photo-induced avalanche pulses shown in Fig.11 are low. Of course, the greater the number of photo-electrons generated by the illumination, the more the avalanche processes triggered by the photo-electrons are.

Considering the self-quenching mechanism, to stop an avalanche process requires a finite time. The accumulation of holes in the potential well requires a few nanoseconds to trigger a sharp decrease in the electric field in the avalanche zone; the time is also required for the process, by which the holes from the P-enriched region diffuse into the substrate and drift toward the back electrode and the drift rings. When the pulsed light is modulated too rapidly, the self-quenching process and the sequential avalanche process probably have no enough time to finish, hence the avalanche pulse counts at the high frequency (above 1 MHz) are degraded as shown in Fig. 12.

According to the above discussion, some conclusions on the presented backside-illuminated ADD can be obtained as follows.

1) The avalanche process is quenched by the change in high electric field, which affects the gain for avalanche multiplication.

2) The avalanche multiplication is not independent of the active region and the substrate. There are many holes and a large bulk leakage current in the depleted bulk.

3) Most photo-electrons do not enter into the high electric field zone, thus they cannot effectively trigger the avalanche multiplication.

4) A long time is required to quench an avalanche process.

Because the photo-electrons are generated in the depleted bulk and drift towards the central region to trigger avalanche multiplication, the structure of the avalanche junction must be a heavily doped N^+ region surrounded by a lightly doped P region. In practice, it is too difficult to control the critical conditions of the lightly doped P region that is fully depleted while the central P–N junction is operated in Geiger mode. The large hole current flows to the depleted bulk from the P region, or the P region is partially depleted and is still neutral. Therefore, the photo-electrons generated in the depleted bulk barely enter into the high electric field of the central P–N junction and trigger the avalanche multiplication.

These limitations obtained from the research of the MPI and the NDL restrict the development of the backside-illuminated ADD. The improvement on the fill factor through fabricating a novel SiPM integrated by the backside-illuminated ADDs is not easy to realize. If the critical conditions could be controlled appropriately during the fabrication and the application, and if the structure could be adopted that the multiplied holes transporting in the avalanche region are independent of the collection of photo-electrons, an excellent backside-illuminated ADD could be fabricated.

7. Conclusions

To improve the PDE of SiPM, the concept of the backside-illuminated silicon ADD is investigated as a basic building-block of SiPM. Because of the creative structure, the backside-illuminated silicon ADD promises a high PDE over the full wavelength range of optical photons and even for ultraviolet light and X-ray.

A newly developed backside-illuminated silicon ADD is designed and fabricated at the NDL using silicon planar technology including ion implantation and double-sided lithography with infrared alignment. Simulations of the electrostatic potential distribution, the electric field distribution, and the current density distribution are performed by using ISE-TCAD. For the fabricated and encapsulated detector, the electrical and photoelectric performances are tested. On the ba-

sis of the device physics and the preliminary results from the NDL and the MPI, some limitations and prospects in the development of the backside-illuminated ADD are presented and analyzed.

References

[1] Musienko Y 2009 *Nucl. Instrum. Method A* **598** 213

[2] Gomi S, Hano H, Iijima T, Itoh S, Kawagoe K, Kim S H, Kubota T, Maeda T, Matsumura T, Mazuka T, Miyabayashi K, Miyata H, Murakami T, Nakadaira T, Nakaya T, Otono H, Sano E, Shinkawa T, Sudo Y and Takeshita T 2007 *Nucl. Instrum. Method A* **581** 427

[3] Ninković J 2007 *Nucl. Instrum. Method A* **580** 1020

[4] Liu Y, Wu Q L, Han Z F, Dai Y M and Guo G C 2010 *Chin. Phys. B* **19** 080308

[5] Otte N 2006 *Proc. IX International Symposium on Detectors for Particle, Astro particle and Synchrotron Radiation Experiments, SNIC Symposium*, April 3–6, California, USA, p. 1

[6] Zhang G Q, Hu X B, Hu C Z, Yin D P, Liang K, Yang R and Han D J 2010 *Nucl. Instrum. Method A* **621** 116

[7] Moser H G, Hass S, Merck C and Ninkovic J 2007 *International Workshop on New Photon-Detectors PD*07, June 27–29, Kobe, Japan p. 5

[8] Lutz G, Otte N, Richter R H and Strüder L 2005 *IEEE Trans. Nucl. Sci.* **52** 1156

[9] Ninković J, Eckhart R, Hartmann R, Holl P, Koitsch C, Lutz G, Merck C, Mirzoyan R, Moser H G, Otte A N, Richter R, Schaller G, Schopper F, Soltau H, Teshima M and Vâlceanu G 2007 *Nucl. Instrum. Method A* **580** 1013